Self-focusing of femtosecond diffraction-resistant vortex beams in water

Stacy Shiffler,[1] Pavel Polynkin,[2,*] and Jerome Moloney[2,3]

[1]*Department of Physics, University of Arizona, Tucson, Arizona 85721, USA*

[2]*College of Optical Sciences, University of Arizona, Tucson, Arizona 85721, USA*

[3]*Department of Mathematics, University of Arizona, Tucson, Arizona 85721, USA*

**Corresponding author: ppolynkin@optics.arizona.edu*

Received August 8, 2011; revised August 31, 2011; accepted August 31, 2011; posted September 2, 2011 (Doc. ID 152567); published September 23, 2011

We report experiments on self-focusing of femtosecond diffraction-resistant vortex beams in water. These beams are higher-order Bessel beams with weak azimuthal modulation of the transverse intensity patterns. The modulation overrides the self-focusing dynamics and results in the formation of regular bottlelike filament distributions. The peak-power thresholds for filamentation, at a particular distance, are relatively accurately estimated by the adaptation of the Marburger formula derived earlier for Gaussian beams. The nonlinear conversion of the incident conical waves into the localized spatial wave packets propagating near the beam axis is observed.

OCIS codes: 190.5940, 190.7110, 050.4865.

Ultrafast laser filamentation is an interdisciplinary field of modern physics that deals with the propagation of ultraintense laser pulses in transparent dielectrics [1–3]. Most of the practical applications of filamentation are based on the properties of laser filaments in gases. However, transparent condensed media offer a convenient platform for experimental studies of filamentation, because the power threshold for self-focusing in this case is three orders of magnitude lower.

Early on in filamentation studies, it was realized that beam shaping offers an effective means of control over the extent of the generated filaments and their placement within the beam profile. The application of various beam shapes to filament formation, in both gaseous and condensed media, has been extensively studied in the past. Examples of beams previously used for the formation of filaments with particular properties include fundamental Bessel beams [4,5], vortex beams [6–8], necklace beams [9], and self-bending Airy beams [10,11].

In this Letter, we report experiments on filamentation of femtosecond diffraction-resistant vortex beams in water. These beams are obtained by imposing a weak azimuthal intensity modulation onto truncated Bessel beams of higher order. The bottlelike intensity distributions of these beams are maintained on propagation over extened distances.

Ideal higher-order Bessel beams have their transverse amplitudes proportional to $J_n(2\pi r/r_0)\exp(in\theta)$, where J_n is the nth-order Bessel function of the first kind, n is the beam order, (r, θ) are transverse polar coordinates, and r_0 is a scale factor. Bessel beams with an order of one or larger have zero on-axis intensity. The diameter of their dominant intensity ring increases with the beam order. These beams are generated through the following phase-only beam amplitude modulation of an incident plane wave [12]:

$$T_n(r,\theta) = \exp(in\theta)\exp\left(-\frac{2\pi i r}{r_0}\right). \quad (1)$$

The ideal Bessel beam of the nth order is an optical vortex with charge n. It has been shown previously that if such a beam has an intensity sufficient for self-focusing, it will break up into $(2n+1)$ filaments positioned evenly along the dominant ring intensity feature of the beam [7,8].

The beams that we use in our experiments are obtained though the amplitude modulation in the form [Eq. (1)] imposed onto an incident femtosecond Gaussian beam. In our setup, the modulation function is defined modulo 2π. The azimuthal component of the phase for the nth-order beam experiences exactly n 2π-jumps along the circumference of the beam. The phase is not defined at these n equidistantly spaced jump points. Coupled to the ultrafast nature of the pulse, this results in the weak azimuthal modulation of the generated higher-order Bessel beams. Such modulation is universal for 2π-modulo phase masks if they are applied to ultrashort optical pulses with a duration comparable to one optical period. As we will show, the azimuthal modulation of the beam patterns in our case completely overrides the self-focusing dynamics and results in the generation of n filaments for the nth-order beam, instead of the $(2n+1)$ filaments to be expected for the ideal nth-order Bessel beam. We point out that although we will refer to the beams used in our experiments as J_n, the properties of these beams in the nonlinear regime are significantly different from those of the ideal higher-order Bessel beams, due to the azimuthal intensity modulation.

The experimental setup used for the studies of filamentation of diffraction-resistant optical vortices in water is schematically shown in Fig. 1. The input Gaussian beam with an 18 mm beam diameter is generated by a commercial ultrafast Ti:sapphire-based amplifier that operates at 10 Hz pulse repetition frequency and outputs 40 fs long pulses with a center wavelength of 800 nm. The input beam pattern is phase-modulated by a computer-controlled, reflective spatial light modulator (SLM, model X10468 by Hamamatsu Photonics). The SLM matrix has 600×800 pixels, and its clear aperture is 12 mm by 16 mm; thus it slightly clips the incident beam in both

0146-9592/11/193834-03$15.00/0

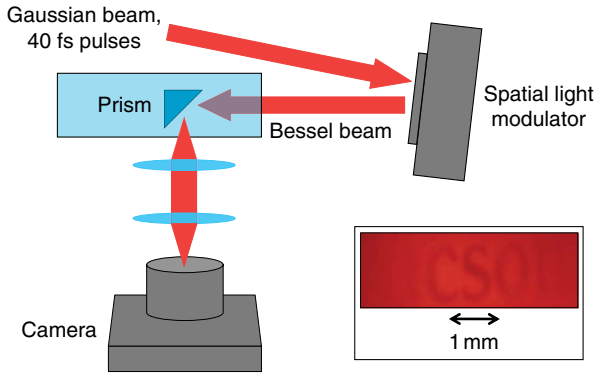

Fig. 1. (Color online) Schematic of the experimental setup. The inset shows the word "Tucson" that was printed on the surface of the prism and imaged onto the camera. From this image, the imaging depth is estimated at about 1 mm.

horizontal and vertical dimensions. The SLM did not show any signs of damage through the continuous exposure to the incident laser beam at the highest pulse-energy level of 3 mJ.

The self-focusing and filamentation of the modulated beams takes place in a glass-walled cuvette filled with distilled water. The size of the cuvette is 1.6 mm × 2.0 mm × 7.6 mm, and its length is chosen to be approximately equal to the dispersion length of the laser pulses in water. The distance between the entrance window of the cuvette and the SLM is 16 cm. For the particular realizations of the vortex beams that we use, the entire length of the cuvette is well within the diffraction-resistant zone of the beams.

To image the transverse intensity distribution of the beam propagating in the water, we immerse a small glass prism into the beam path. The uncoated glass surface of the prism reflects about 1.3% of the incident *s*-polarized beam. The reflected light is imaged onto a digital camera and photographed. For the imaging to be linear, it is important that the reflection off the prism surface is sufficiently small. The prism is translated along the beam path, which allows us to visualize the beam evolution on propagation through the water.

In Fig. 2, we show the transverse intensity patterns imaged at a 5 mm distance from the entrance to the water cell, for selected beam orders. The radial part of the phase modulation imposed by the SLM, for all cases shown, is such that the total cumulative phase shift from the center of the beam to the edge equals 100π. The azimuthal component of the modulation varies depending on the beam order according to Eq. (1). The peak power of the laser pulses is substantially below the self-focusing threshold; thus the beams propagate in the linear regime.

It is evident that the ring intensity features of the beams, which are supposed to be smooth for the case of ideal Bessel beams, are modulated. There are exactly

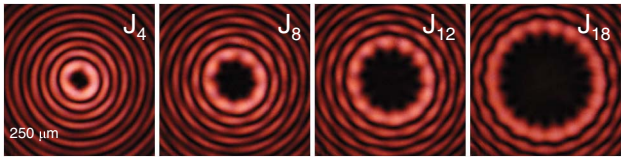

Fig. 2. (Color online) Examples of the experimentally generated beams in the linear propagation regime (at low intensity).

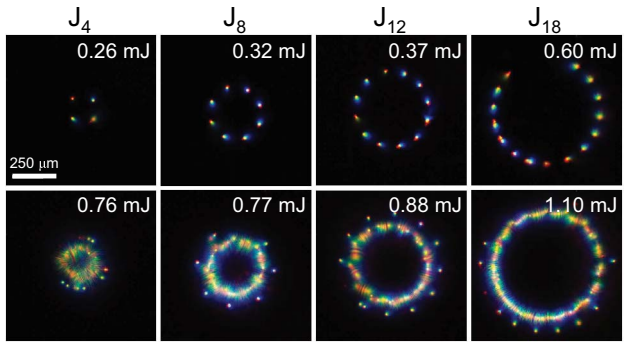

Fig. 3. (Color online) Top row: Images of the white-light emission at the pulse-energy levels corresponding to the onset of filamentation at 5 mm from the entrance to the water cuvette, for selected beam orders. Bottom row: Same as above, at the energy levels corresponding to the onset of filamentation in the secondary ring intensity features.

n intensity beads (or hot spots) along the circumference of the ring intensity features of the beam of nth order. The peak-to-peak amplitude of the intensity modulation of the dominant ring, relative to its mean value, is between 10% and 20%, depending on the beam order. The beaded structure of the beams is due to the 2π-modulo mask used coupled with the ultrashort nature of the input pulses, as discussed above.

When the pulse energy is increased, distinct filaments start forming on the dominant intensity rings of the beams. The placement of filaments is determined by the azimuthal intensity modulation of the ring features. There are n filaments formed on the nth-order beam. The self-focusing collapse is accompanied by the emission of the forward-propagating white-light continuum radiation [1–3]. In the top row of Fig. 3, the white-light continuum is imaged at the pulse-energy levels at which the filamentation starts to occur at a 5 mm distance from the entrance to the water cell. These images are taken through a color-glass filter that allows visible light to pass through but blocks the pump light at 800 nm. As the pulse energy is increased further, filaments start forming on the secondary rings of the beams, as shown in the bottom row of Fig. 3.

For bell-shaped beams, the peak-power threshold P_{th} for filamentation, at a particular distance L_c, can be relatively accurately estimated using the semiempirical Marburger formula [13]:

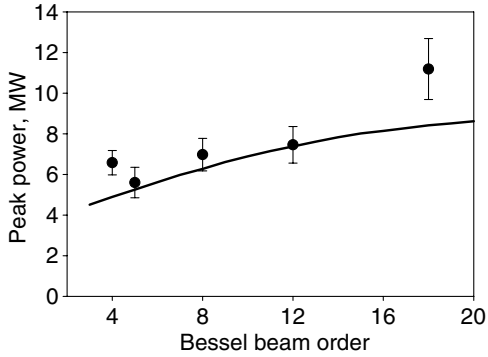

Fig. 4. Critical power for filamentation for the diffraction-resistant vortex beams. Experimental data points are shown with circles. The solid line is the result of the calculation based on the adaptation of the Marburger formula.

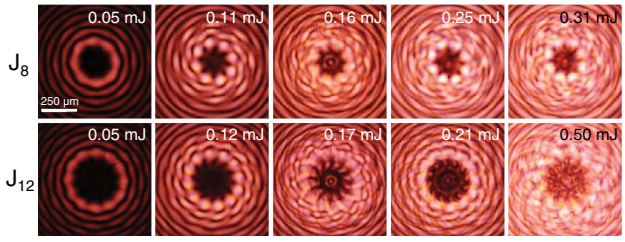

Fig. 5. (Color online) Beams of order 8 (top row) and 12 (bottom row) imaged at 50 mm from the entrance to the water cuvette, at various pulse energies.

$$L_c = \frac{0.367\pi n_0 w_0^2}{\lambda_0 \sqrt{[(P_{\mathrm{th}}/P_{\mathrm{cr}})^{1/2} - 0.852]^2 - 0.0219}}, \qquad (2)$$

where w_0 is the input beam radius, λ_0 is the wavelength of the pump beam in a vacuum, n_0 is the linear refractive index of the medium, and P_{cr} is the critical power for self-focusing at infinity, which for water approximately equals 4 MW [14]. This formula can be adapted for the estimation of the filamentation thresholds for the diffraction-resistant vortex beams at a particular propagation distance. In our case, the power in the dominant intensity ring of the nth-order beam is approximately equally partitioned between the n formed filaments, and w_0 is approximately equal to the half-width of the ring. The fraction of power in the center ring is deduced from the numerical solution of the Fresnel diffraction integral. The result of the calculation following this procedure, for the case of $L_c = 5$ mm, is shown in Fig. 4 with a solid curve. The experimental data for selected beam orders is in reasonably good agreement with the calculation. Within the experimental error, the threshold peak power grows with the beam order.

As the self-focusing beams propagate further into the water cell, the intensity ring features of the beams self-focus as a whole, at the same time as the breakup of the rings into individual filaments occurs. In addition, the nonlinear conversion of the conical waves from the incident beam into various spatial wave packets propagating near the beam axis takes place. A similar effect has been previously reported for the case of self-focusing of the fundamental Bessel beam [15]. The detailed study of these complex dynamics, examples of which are shown in Fig. 5, is an interesting and challenging problem, but it is beyond the scope of the work reported here.

In summary, we have studied the filamentation of femtosecond diffraction-resistant vortex beams in water. Regular filament patterns have been found to form on the dominant intensity rings of the beams. The placement of filaments within the transverse beam profile was dominated by the azimuthal amplitude modulation imposed by the 2π-modulo phase mask used to generate the beams. The pulse-energy thresholds for the onset of filamentation, at a particular propagation distance, have been relatively accurately estimated by the adaptation of the Marburger formula. The nonlinear conversion of the incident conical waves into localized wave packets propagating near the beam axis has been observed.

The authors acknowledge support from the United States Air Force Office of Scientific Research (USAFOSR) under programs FA9550-10-1-0237 and FA9550-10-1-0561.

References

1. A. Couairon and A. Mysyrowicz, Phys. Rep. **441**, 47 (2007).
2. L. Bergé, S. Skupin, R. Nuter, J. Kasparian, and J.-P. Wolf, Rep. Prog. Phys. **70**, 1633 (2007).
3. S. L. Chin, *Femtosecond Laser Filamentation* (Springer, 2010).
4. A. Dubietis, P. Polesana, G. Valiulis, A. Stabinis, P. Di Trapani, and A. Piskarkas, Opt. Express **15**, 4168 (2007).
5. P. Polynkin, M. Kolesik, A. Roberts, D. Faccio, P. Di Trapani, and J. Moloney, Opt. Express **16**, 15733 (2008).
6. M. S. Bigelow, P. Zerom, and R. W. Boyd, Phys. Rev. Lett. **92**, 083902 (2004).
7. A. Vinçotte and L. Bergé, Phys. Rev. Lett. **95**, 193901 (2005).
8. L. T. Vuong, T. D. Grow, A. Ishaaya, A. L. Gaeta, G. W. 't Hooft, E. R. Eliel, and G. Fibich, Phys. Rev. Lett. **96**, 133901 (2006).
9. T. D. Grow, A. I. Ishaaya, L. T. Vuong, and A. L. Gaeta, Phys. Rev. Lett. **99**, 133902 (2007).
10. P. Polynkin, M. Kolesik, J. V. Moloney, G. A. Siviloglou, and D. N. Christodoulides, Science **324**, 229 (2009).
11. P. Polynkin, M. Kolesik, and J. Moloney, Phys. Rev. Lett. **103**, 123902 (2009).
12. C. Paterson and R. Smith, Opt. Commun. **124**, 121 (1996).
13. J. H. Marburger, Prog. Quant. Electr. **4**, 35 (1975).
14. Z. W. Wilkes, S. Varma, Y.-H. Chen, H. M. Milchberg, T. G. Jones, and A. Thing, Appl. Phys. Lett. **94**, 211102 (2009).
15. R. Gadonas, V. Jarutis, R. Paškauskas, V. Smilgevičius, A. Atabinis, and V. Vaičaitis, Opt. Commun. **196**, 309 (2001).